New York Journal of Mathematics

New York J. Math. **28** (2022) 367–401.

Unoriented Khovanov Homology

Scott Baldridge, Louis H. Kauffman and Ben McCarty

ABSTRACT. The Jones polynomial and Khovanov homology of a classical link are invariants that depend upon an initial choice of orientation for the link. In this paper, we give a Khovanov homology theory for unoriented virtual links. The graded Euler characteristic of this homology is proportional to a similarly-defined unoriented Jones polynomial for virtual links, which is a new invariant in the category of non-classical virtual links. The unoriented Jones polynomial continues to satisfy an important property of the usual one: for classical or even virtual links, the unoriented Jones polynomial evaluated at one is two to the power of the number of components of the link. As part of extending the main results of this paper to non-classical virtual links, a new framework for computing integral Khovanov homology based upon arc-labeled diagrams is described. This framework can be efficiently and effectively implemented on a computer. We define an unoriented Lee homology theory for virtual links based upon the unoriented version of Khovanov homology.

CONTENTS

1. Introduction 367
2. Unoriented Jones polynomial for classical inks 371
3. Unoriented Jones polynomial for virtual links 373
4. Bracket homology and Khovanov homology 384
5. Bracket homology of virtual links 387
6. Unoriented Khovanov homology 394
7. Lee homology of unoriented links 397
8. Future aims 398
References 399

1. Introduction

It is well-known that the Kauffman bracket polynomial does not require the choice of an orientation on the link. However, the Jones polynomial and Khovanov homology based upon it does. The same is true for virtual links: The Khovanov homology defined in [8, 27] is an *oriented* virtual link invariant. In

Received June 15, 2021.

2020 *Mathematics Subject Classification.* 57K10, 57K12, 57K14, 57K18.

Key words and phrases. unoriented, Khovanov homology, virtual link, knot, Jones polynomial, Lee homology, parity, core, mantle, multicore decomposition.

ISSN 1076-9803/2022

this paper, we show how to get polynomial and homology invariants of the underlying link that are independent of the orientation.

In the original Khovanov invariants, the orientation was used to determine an overall grading shift in the bracket homology (cf. Theorem 4.2 and Theorem 5.6). (The bracket homology is the "categorification" of the Kauffman bracket of a diagram.) We introduce appropriate grading shifts that also lead to an invariant homology that does not require L to be oriented. To describe these shifts, we need three numbers for any virtual diagram: s_+, s_-, and m. The number m is the number of *mixed-crossings* of the diagram, i.e., the number of classical crossings between different components of the link. Each component can also have several *self-crossings*. The self-crossings bifurcate into two types, s_+ and s_-, that correspond to the number of positive and negative self-crossings of the diagram.

Let $(C(D), \partial)$ be the bracket complex defined in Section 4 for a diagram D of an unoriented link L. The unoriented Khovanov chain complex, $\tilde{C}(D)$, is a gradings-shifted version of the bracket complex:

$$\tilde{C}(D) = C(D)[-s_- - \frac{1}{2}m]\{s_+ - 2s_- - \frac{1}{2}m\}.$$

Here the first grading shift is for the homological grading and the second is for the q-grading of the bi-graded complex. The homology of this complex, called *unoriented Khovanov homology*, is an invariant of the link (cf. Theorem 6.1):

Theorem 6.1. *Let L be an unoriented virtual link. The unoriented Khovanov homology, denoted $\widetilde{Kh}(L)$, can be computed from any virtual diagram of L and is a virtual link invariant.*

For a classical link, the unoriented Khovanov homology can be defined directly from an unoriented link diagram (cf. Section 4). For virtual links, the present definition of the chain complex requires an initial choice of an orientation for the link diagram. The chain complex is, up to isomorphism, independent of the choice of orientation. In this sense our homology is unoriented. It remains an open problem how to define the chain complex without choosing an orientation for the link diagram when the link is virtual.

Question 1.1. *For virtual links, can unoriented Khovanov homology be defined directly from an unoriented link diagram without ever choosing an orientation?*

The bracket homology and grading-shifts also lead to an unoriented version of Lee homology:

Theorem 7.1. *Let L be an unoriented virtual link. The unoriented Lee Homology, $Kh'(L)$, is an invariant of the link L.*

The proofs of Theorem 6.1 and Theorem 7.1 start by calculating the bracket homology $H(D)$, of the bracket complex $C(D)$, associated to a link diagram D, and then shifting gradings appropriately to get an invariant of the link L (cf. Section 4 and Section 5).

In order to obtain an integral version of Khovanov homology for virtuals, a number of problems had to be overcome. The fact that states differing in only one smoothing can have the same number of loops (see Figure 6) presents a new phenomenon not seen in classical links. This phenomenon leads to the need to use a local coefficient system to define the differential in the chain complex for this version of Khovanov homology (cf. [8]). The local coefficient system demands the use of base points for the algebra and then the articulation of paths in the state loops from the base points to the sites where algebra operations are performed (to find boundaries in the chain complex). On these paths we count the parity of the number of cut points (another structure on the diagram) to effect the algebra transformation for the local coefficients. All of this then requires a global ordering, local orderings, cut point choices and base point choices. It is proved that the resulting homology is independent of all these choices (cf. [8]). But it is important to find a way to make these choices in a natural way that lets one work with and compute with this structure. In this paper we use arc-labeled diagrams (D, A) where the A denotes a choice of labeling on the arcs of the diagram D (defined in Section 5). Thus we obtain,

Theorem 5.4. *Let (D, A) be an arc-labeled diagram for a virtual link L. The arc labels determine a differential*

$$\partial^i_A : C^{i,j}(D) \to C^{i+1,j}(D)$$

and form $(C^{i,j}(D), \partial_A)$ into a chain complex. Furthermore, if A' is another arc labeling for the same diagram D, then $H^{i,j}(D, A) \cong H^{i,j}(D, A')$.

Until now, this additional structure was chosen manually by inspecting a diagram and making judgments as to where to place the base points, cut points, etc. on the diagram. There was no standard, algorithmic process for determining these choices, which, in our observations, formed an artificial barrier to working with Khovanov homology of virtual links for the last decade. Thus, the arc labeling standardizes these choices, and makes it possible to handle the chain complex both theoretically and practically. The main content of Theorem 5.4 is that now in order to calculate the virtual Khovanov homology you simply need to *choose an arc labeling for the diagram* and then every other choice is determined. Furthermore, the fact that arc-labeled diagrams correspond to a standard method of encoding knots make them particularly useful from a programming perspective.

While the virtual link is unoriented, the arc-labeled diagram provides an orientation (see Question 1.1). Another consequence of Theorem 5.4 is that the bracket homology is independent of orientations on a given diagram. Furthermore, we show in Theorem 5.6 that the bracket homology is isomorphic to Khovanov homology and unoriented Khovanov homology up to a grading shift.

An immediate consequence of Theorem 6.1 and Proposition 4.1 is that the graded Euler characteristic of the unoriented Khovanov homology defines a

polynomial invariant that does not depend on the orientation of the link:

$$\chi_q(\widetilde{Kh}(L)) = \sum_{i,j\in\frac{1}{2}\mathbb{Z}} (-1)^i q^j \dim(\widetilde{Kh}^{i,j}(L)).$$

One might reasonably call this the "unoriented Jones polynomial" for the link (see J^0_L in Section 3). However, this choice has two substantial deficiencies. First, the polynomial has complex, not real, coefficients. Second, even for classical links, evaluating the polynomial at $q = 1$ is not always positive as it is for the usual Jones polynomial. A significant amount of this paper is dedicated to correcting both of these deficiencies. It turns out that the solution—cores and mantles—can be applied to fix other problems that have come up in the virtual link theory literature.

We can get a hint of how to fix these deficiencies by looking at classical links. For classical links, the required normalization is to multiply $\chi_q(\widetilde{Kh}(L))$ by $(-1)^\lambda$ where $\lambda = \sum_{i<j} Lk(K_i, K_j)$. (Note that this normalization does require choosing an orientation, but in Section 2 we show that $(-1)^\lambda$ is independent of that choice.) In Section 3, we define a generalization of λ, denoted $\tilde{\lambda}$, based upon a modified linking number between different components. This number, which is equal to the original λ when the link is classical, solves the first deficiency:

Theorem 3.19. *The unoriented Jones polynomial, defined by*

$$\widetilde{J}_L(q) = (-1)^{\left(\tilde{\lambda}-s_- -\frac{1}{2}m\right)} q^{\left(s_+ -2s_- -\frac{1}{2}m\right)} \langle L\rangle,$$

is an unoriented virtual link invariant. Moreover, $\widetilde{J}_L \in \mathbb{Z}[q^{-\frac{1}{2}}, q^{\frac{1}{2}}]$.

The definition of $\tilde{\lambda}$ also solves the second deficiency. An *even link* is a virtual link in which there are an even number of classical mixed-crossings for every component in a diagram of the link (cf. [13, 14, 32]). Even links are sometimes called 2-colorable links in the literature (cf. [37]). Since all virtual knots and classical links are even, one can often generalize theorems of virtual knots and classical links to even virtual links. The next theorem is new in the literature for the usual (oriented) Jones polynomial for *non-classical* virtual links L. It also shows that $\tilde{\lambda}$ correctly addresses the second issue for the unoriented Jones polynomial (see the following and Corollary 3.24):

Theorem 3.23. *If L is an oriented virtual link with ℓ components, then*

$$\widetilde{J}_L(1) = J_L(1) = \begin{cases} 2^\ell & \text{if } L \text{ is even} \\ 0 & \text{if } L \text{ is odd.} \end{cases}$$

The number, $J_L(1)$, is independent of the choice of orientation.

Thus, we prove that the usual (oriented) Jones polynomial, J_L, counts the number of components of a virtual link when the link is even, extending this well-known property for classical links, and that the unoriented Jones polynomial, $\widetilde{J}_L$, also preserves this property.

Remark 1.2. *Aspects of Theorem 3.19 and Theorem 3.23 have been known about classical links since Jones. Morton gave a specific formula for the change in the Jones polynomial under change in orientation of a component [33]. His argument was based on the skein relation and prior to the discovery of the bracket model. The bracket model and the Markov trace models make such formulae straightforward to deduce in the classical case. We have returned to this subject in the nontrivial case of virtuals and Khovanov homology.*

In order to define $\widetilde{\lambda}$, we needed to introduce a new idea in virtual link theory that extends even link invariants to all virtual links: the identification of the *core* and *mantle* of a virtual link, and more generally, a *multi-core decomposition* (See Section 3.2). A multi-core decomposition is the separation of a virtual link L into a set of invariant sub-links, $L = C_1 \cup ... \cup C_n \cup M_n$, where each sub-link C_i is even (C_1 is called *the* core), and the sub-link M_n is either the empty link, or it is odd (M_n is the final mantle).

While there are a number of invariants for even virtual links in the literature, generalizing them to all virtual links has been elusive. They fail to be invariants for odd virtual links because the definition of the invariant often depends heavily on each component having an even number of classical mixed-crossings. By identifying an invariant even sub-link, the core, and eventually a set of invariant even sub-links in the multi-core decomposition, one can derive an invariant of odd links by applying the even link invariants to each even core in the decomposition.

Theorem 3.8. *Any invariant of even links, Ψ, induces a tuple of invariants*

$$(\Psi(C_1), ..., \Psi(C_n))$$

for the multi-core decomposition of a virtual link L, and the tuple itself is an invariant.

In the case of the unoriented Jones polynomial, the multi-core decomposition identifies a maximal set of maximal even sub-links on which the virtual link "acts like" an even link. Thus, the unoriented Jones polynomial for odd links defined in this paper is the polynomial that is the "closest to" the unoriented Jones polynomial for classical links.

Acknowledgements. Kauffman's work was supported by the Laboratory of Topology and Dynamics, Novosibirsk State University (under contract number 14.Y26.31.0025 with the Ministry of Education and Science of the Russian Federation). All three authors would like to thank William Rushworth for many helpful conversations and suggestions.

2. Unoriented Jones polynomial for classical inks

We introduce the main ideas of this paper by reviewing and generalizing the oriented version of the Jones polynomial for classical links to the unoriented

Jones polynomial. Recall that to get the Jones polynomial, one multiplies the Kauffman bracket by a normalization factor that depends on the writhe, i.e.,

$$J_L(q) = (-1)^{-n_-} q^{n_+ - 2n_-} \langle L \rangle$$

where n_- and n_+ are the number of negative and positive (classical) crossings respectively[1] (cf. [4, 12, 16]). Here we are using the form of the Kauffman bracket given by

$$\langle \times \rangle = \langle \asymp \rangle - q \langle \; \rangle \langle \rangle, \text{and} \tag{1}$$

$$\langle \bigcirc \cup D \rangle = (q^{-1} + q) \langle D \rangle. \tag{2}$$

Clearly, the normalization depends upon the way the components are oriented, but the Kauffman bracket itself does not depend upon a choice of orientation. The new normalization factor is defined as follows. Let $L = K_1 \cup \cdots \cup K_\ell$ be a link with ℓ components and let D be a virtual diagram of L. A *self-crossing* in D is a classical crossing in which both under- and over-arcs of the crossing are from the same component. For a specific component K_i, the usual signs for each self-crossing of K_i are the same for either orientation of K_i. Let s_+ and s_- be the total number of positive and negative self-crossings of a link L.

The first Reidemeister move is covered by the self-crossing data, and the third Reidemeister move does not play a role in any normalization. For the second Reidemeister move, the case of using the move on a single component K_i is taken care of by the self-crossing data. The final case is a Reidemeister two move for strands from two different components of a link. Therefore, the remaining type of crossing to consider is a mixed-crossing: Let m be the total number of mixed-crossings of a diagram D. Note that we do not assign a positive or negative sign to these crossings.

Applying the Kauffman bracket to two strands with one over the other, we see that

$$\langle \; \rangle = -q \langle \; \rangle.$$

In other words, we can pull the strands apart at the cost of multiplying by an overall factor of $-q^{-1}$ (which partially motivates the usual normalization). Note that

$$(-1)^{-\frac{1}{2}m} q^{-\frac{1}{2}m}, \tag{3}$$

yields the proper correction factor to ensure that the polynomial is invariant under a Reidemeister 2 move. Further, note that the change in $-\frac{1}{2}m$ is equal to the change in $n_+ - 2n_-$ under the move because, for any orientation of the strands, there will always be one positive crossing and one negative crossing.

[1] The Jones polynomial is usually written with $(-1)^{n_-}$ instead of $(-1)^{-n_-}$. These are equivalent since n_- is an integer. Later in this paper, we work with half-integer powers of -1 where the negative of a power is not equivalent: $(-1)^{\frac{1}{2}} \neq (-1)^{-\frac{1}{2}}$. In this context, $(-1)^{-n_-}$ is the correct normalization.

Thus we may define the *unoriented Jones polynomial* of a classical link L by

$$\tilde{J}_L(q) = (-1)^{-n_-} q^{\left(s_+ - 2s_- - \frac{1}{2}m\right)} \langle L \rangle. \tag{4}$$

Based upon Expression (3), one should expect to see $-s_- - \frac{1}{2}m$ as the exponent of -1 instead of $-n_-$. However, as we will elaborate in Section 3,

$$n_- = -\lambda + s_- + \frac{1}{2}m, \tag{5}$$

where $\lambda = \sum_{i<j} Lk(K_i, K_j)$. To compute λ requires a choice of orientation. This sum of linking numbers changes by an even number when the orientation of L is changed. Hence, n_- is made up of two terms that do not change under a change of orientation and one term that changes by an even number.

The discussion above immediately implies

Theorem 2.1. *The unoriented Jones polynomial $\tilde{J}_L$ of a classical link L is an invariant of the link.*

Next we extend the definition of the unoriented Jones polynomial to virtual links. There are a number of pitfalls. The first is that $\frac{1}{2}m$ and $Lk(K_i, K_j)$ can be half integers. This means that the polynomial may have imaginary-valued coefficients. Since we wish to preserve (as much as possible) the well known fact that evaluating the Jones polynomial at 1 is 2^ℓ, this presents a problem. Worse yet, if the orientation of K_i (or K_j) is reversed, then $Lk(K_i, K_j)$ changes by an odd number if the total number of mixed-crossings between K_i and K_j is odd. Hence, the term λ needs to be modified to compensate for this issue. We tried many potential modifications that were orientation invariant, however, these modifications could not be normalized so that the well-known fact (2^ℓ) continued to hold, even for classical links. For a discussion about why this might be desired, see the second item in Section 8. The solution involves what we call the "core" of the virtual link, and it turns out that the core has far wider implications for virtual link theory.

3. Unoriented Jones polynomial for virtual links

Before defining the core of a virtual link, we begin this section by recalling some basic facts about virtual link theory.

3.1. Virtual knot theory. Classical knot theory is the study of embeddings of disjoint unions of S^1 in S^3. Virtual knot theory, as introduced by Kauffman [18], is also the study of disjoint unions of S^1, but in a different ambient space: $\Sigma_g \times [0,1]$, where Σ_g denotes a closed orientable surface of genus g. Unlike links in many other 3-manifolds, virtual links have a diagrammatic theory, akin to to that of classical links. We begin by recalling some of the relevant facts about the theory, and refer the reader to [18, 20, 30] for a more thorough treatment.

A virtual link diagram is a 4−valent planar graph in which the vertices are decorated with classical crossings or *virtual crossings*, denoted by $\otimes$. Examples of virtual link diagrams are given in Figure 2 and Figure 12.

Two classical knots are equivalent if and only if their diagrams are related by a finite sequence of the classical Reidemeister moves. Two virtual knots are equivalent if and only if their diagrams are related by a finite sequence of the Reidemeister moves together with the virtual Reidemeister moves. The moves are shown in Figure 1. One may think of the virtual link itself as an equivalence class of virtual link diagrams, each member of which is related to the rest by a finite sequence of classical and virtual Reidemeister moves.

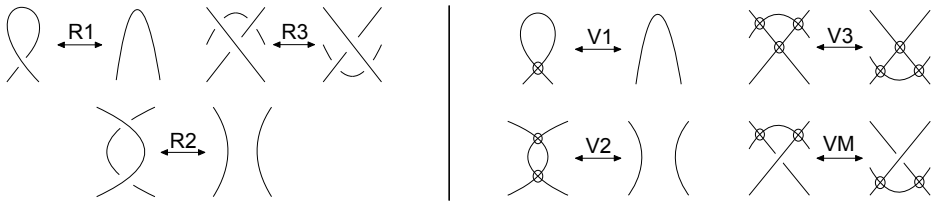

FIGURE 1. The classical and virtual Reidemeister moves.

A classical link diagram is simply a virtual link diagram without virtual crossings. Thus, classical knot theory is a proper subset of virtual knot theory. For an in-depth treatment of the diagrammatic theory of virtual links see [18].

3.2. The even core of a virtual link. For classical links, the Jordan Curve Theorem implies that each component of a link diagram intersects every other component of the diagram in an even number of crossings. However, virtual crossings are not genuine crossings, which allows one to define various parities for virtual links.

Definition 3.1 (Component-to-Component Parity)**.** *Let D be a diagram of a virtual link L with components $K_1, ..., K_\ell$. The* component-to-component parity*, denoted $\pi(K_i, K_j)$, is* 0 *if there are an even number of mixed crossings between components K_i and K_j and* 1 *otherwise.*

Definition 3.2 (Component Parity)**.** *Let D be a diagram of a virtual link L with components $K_1, ..., K_\ell$. Define the parity of K_i, denoted $\pi(K_i)$, to be the number of mixed crossings of D involving component K_i, modulo 2.*

Note that the number of mixed crossings of a component is equal to the number of virtual crossings modulo two.

Definition 3.3 (Link Parity)**.** *Let D be a diagram of a virtual link L with components $K_1, ..., K_\ell$. The link L is called* even *if all components of L are even, i.e., $\pi(K_i) = 0$ for all i, and called* odd *if there exists an odd component. The parity of L, denoted $\pi(L)$, is $\pi(L) = 0$ if L is even and $\pi(L) = 1$ if L is odd.*

Note that the virtual Reidemeister moves have no effect on these parities, and the classical Reidemeister moves clearly leave them unchanged, and hence we obtain:

Lemma 3.4. *The link parity, each component parity, and each component-to-component parity of a link are all virtual link invariants.*

It is well-known that even virtual links form a subset of virtual links for which it is often easier to define invariants (cf. [14,32,37]). However, odd virtual links present certain challenges. Some of these challenges may be overcome by choosing an invariant even sublink.

Definition 3.5. *Given a diagram of a virtual link $L = K_1 \cup K_2 \cup ... \cup K_\ell$ we obtain a sub-link L_1 by deleting all the odd components of L. The resulting sub-link L_1 may be even or odd. If it is even, stop. Otherwise, repeat the procedure on L_1 to get L_2, and continue until an even sub-link, L_k, is obtained (L_k may be the empty link, which is even). Call the even sub-link L_k* the core *of L and denote it by C.*

Note that after deleting the odd components of L_i to get L_{i+1}, it is possible that components of L_{i+1} that were even in L_i become odd in L_{i+1}. Lemma 3.4 still applies to the sub-link L_{i+1} thought of as a link by itself. Therefore the deletion process is unique: L_1 will always be even or odd as its own link, and the odd components of L_1 that are deleted to get L_2 will always be the same components, and so on. Thus, we immediately obtain:

Lemma 3.6. *Any invariant of the even core of a virtual link L is an invariant of L.*

Invariants of odd links calculated from the even core leave out much of the information about the link. In order to recapture some of that information it is helpful to look at the complement of the even core, which we call the *mantle* of the virtual link.

Definition 3.7. *The* mantle *of a link L is the sub-link M given by the complement of the core, i.e., $M = L \setminus C$.*

Note that the mantle may be either an even or odd link in its own right, and possesses its own even core. Hence, we may repeat the process described above. Given a virtual link L, determine its core C_1 and mantle, M_1 ($L = M_1 \cup C_1$) using Definition 3.5. Next, determine the core of M_1 and denote it by C_2 using Definition 3.5. This process also determines a new mantle, M_2. At this stage, $L = C_1 \cup C_2 \cup M_2$. Repeat this process until M_n is either empty or has an empty core (if M_n is non-empty and has empty core, it must contain only odd components). Thus, one obtains a decomposition of the link: $L = C_1 \cup ... \cup C_n \cup M_n$. We call this the *multi-core decomposition* of the link. Repeated applications of Lemma 3.6 yield the following theorem.

Theorem 3.8. *Any invariant of even links, Ψ, induces a tuple of invariants*

$$(\Psi(C_1), \dots, \Psi(C_n))$$

for the multi-core decomposition of a virtual link L, and the tuple itself is an invariant of L.

In particular, this theorem implies that any invariant of even links immediately generalizes to a new invariant of *all* virtual links—not just even links. For example, the papers [32] and [14] generalize the odd writhe of a virtual knot [19] to even virtual links. In [14], a virtual orientation is described where the orientation of a component changes direction in a diagram D at every virtual crossing (which is why the link must be even). Using this orientation, the sum of the signs of classical crossings between K_i and K_j whose over arc is K_i is denoted $\Lambda_D(i,j)$. Clearly, this number depends upon the order: $\Lambda_D(i,j) \neq \Lambda_D(j,i)$ in general.

Corollary 3.9. *[cf. Theorem 14 of [14], see also [32]] Let $L = K_1 \cup K_2 \cup \cdots \cup K_\ell$ be an ordered virtual link. Every core C_r inherits an ordering from the ordering of L. For every core C_r of L, and any pair of components, K_i and K_j in C_r, the number $|\Lambda_{C_r}(i,j)|$ is an invariant of the ordered unoriented virtual link L.*

Another generalization of the odd writhe to even links was given in [37]. In that paper, an even link is equivalent to the link being 2-colorable. The definition of 2-color writhe, $J^2(D)$, of an even link diagram D depends upon a special parity function on each crossing that satisfies the parity axioms (briefly mentioned below). For a given 2-coloring of an oriented link, define a quantity for that coloring as the sum of classical crossing signs of only the odd crossings (where odd is defined by that parity function). The 2-color writhe of the link, $J^2(L)$, is then a tuple of these numbers—one for each 2-coloring of a diagram D of L. This tuple is defined up to permutations of the entries.

Corollary 3.10. *The tuple, $\left(J^2(C_1), \ldots, J^2(C_n)\right)$, consisting of the 2-color writhe of each core is an invariant of the oriented virtual link L.*

Rushworth shows that for a virtual knot, $J^2(K)$ is the odd writhe of K (see Proposition 3.4 of [37]).

Sometimes these tuples of invariants can be profitably added together to get an overall invariant of the link. We want more, however. For an upgraded definition of λ for all virtual links (not just even links), we wish to define "linking numbers" for all components, not just components in each of the cores. To do so, we introduce a parity function defined from pairs of components of L. This parity function is defined on components, but could be described as a parity function on crossings (cf. [31], and [28], [37]), as we will see next.

3.3. A parity function. It will be useful to define a parity function on pairs of components of a virtual link. Let $L = K_1 \cup \ldots \cup K_\ell$ be a virtual link with multi-core decomposition, $L = C_1 \cup C_2 \cup \ldots \cup C_n \cup M_n$. We define a *component parity function* on pairs of components as follows:

$$p(K_i, K_j) = \begin{cases} 0 & K_i, K_j \in C_r \text{ for some } r \\ 1 & \text{otherwise.} \end{cases} \tag{6}$$

This component parity function descends to a parity function on crossings, as described in [31] and [37]. If c is a crossing between component K_i and K_j, then

we assign the parity, $p(K_i, K_j)$, to c. Any self-crossing is assigned a parity of 0. Axioms 0 and 1 (cf. [37]) are clearly satisfied. Because all crossings between K_i and K_j will have the same parity, Axiom 2 is clearly satisfied. For a Reidemeister 3 move, we either have all three components in the same core, C_r, two in the same core, and one is not, or, no two of the strands are in the same core. These correspond to the three allowable cases of Axiom 3. We could just work with the parity function on crossings, but find it convenient to work with the component parity function at the level of component-to-component for reasons that will become apparent below.

3.4. The unoriented Jones polynomial of a virtual link. We wish now to generalize the unoriented Jones polynomial (Equation (4)) for classical links to an invariant of unoriented virtual links. In fact, the same definition together with Equation (5) works for any even virtual link. Here is why: Suppose the orientation of K_i is reversed. In the classical case, the number of mixed crossings between K_i and each other component will be even. For an even virtual link, it is possible that the number of mixed crossings between K_i and K_j is odd for some j (cf. Figure 12). In that case, reversing the orientation on K_i will change $Lk(K_i, K_j)$ by an odd number. However, in an even virtual link, $\pi(K_i) = 0$ for all i. Hence, there must be an even number of components that intersect K_i in an odd number of mixed crossings. Thus, the overall parity of the exponent on (-1) is unchanged by the orientation swap.

For an odd virtual link, the unoriented Jones polynomial as defined for even/classical links need not be an orientation invariant, as the following example shows.

Example 3.11. Let L_0 and L_1 be the oriented virtual Hopf links shown on the left and right, respectively in Figure 2. Observe that unoriented Jones polynomial defined for classical links is not orientation invariant, because $\lambda - s_- - \frac{1}{2}m$ for L_0 is -1 while for L_1 it is 0.

FIGURE 2. Virtual Hopf links with two different orientations.

Thus, we need to extend the unoriented Jones polynomial defined for classical/even links to odd links. This amounts to redefining the term λ. We do this next. Consider a diagram of an oriented virtual link $L = K_1 \cup ... \cup K_\ell$.

We first define a *modified linking number*:

$$\widetilde{Lk}(K_i, K_j) := (-1)^{p(K_i,K_j)\cdot\left(Lk(K_i,K_j)+\frac{1}{2}\pi(K_i,K_j)\right)} Lk(K_i, K_j),$$

where $p(K_i, K_j)$ is the component parity function and $\pi(K_i, K_j)$ is the component-to-component parity. Suppose L has multi-core decomposition $L = C_1 \cup ... \cup C_n \cup$

M_n. The modified linking number is, up to sign, the ordinary linking number, and if K_i and K_j belong to the same core, C_r, it has the same sign as the ordinary linking number. If K_i and K_j belong to different cores, or if at least one of them belongs to the mantle, M_n, then the modified linking number may have the opposite sign as the ordinary linking number.

Lemma 3.12. *The modified linking number, $\widetilde{Lk}(K_i, K_j)$, is an element of $\frac{1}{2}\mathbb{Z}$ and is an oriented virtual link invariant.*

Proof. Consider a diagram of an oriented link L, and a multi-core decomposition $L = C_1 \cup ... \cup C_n \cup M_n$. If K_i and K_j belong to the same core, then the modified linking number is the ordinary linking number and is an integer since each core is an even sub-link.

If K_i and K_j do not belong to the same core, but they do interact in an even number of mixed-crossings, then $\widetilde{Lk}$ is still an integer. Otherwise, K_i and K_j interact in an odd number of mixed-crossings. Thus $Lk(K_i, K_j)$ is a half-integer, and because $\pi(K_i, K_j) = 1$ in this case, the exponent on -1 in the definition of $\widetilde{Lk}$ will be an integer.

The fact that $\widetilde{Lk}$ is an oriented virtual link invariant follows from the fact that the ordinary linking number and parity are link invariants. □

We can use the modified linking number to extend λ from even links to all virtual links:

$$\tilde{\lambda}(L) = \sum_{1 \le i < j \le \ell} \widetilde{Lk}(K_i, K_j). \tag{7}$$

Since $\tilde{\lambda}$ is defined in terms of linking numbers, which are invariant under the Reidemeister moves (virtual and classical), we immediately obtain:

Lemma 3.13. *The number $\tilde{\lambda}$ is an oriented virtual link invariant.*

Remark 3.14. *When L is even, L is the core. Thus, for an even link L, $\lambda = \tilde{\lambda}$ and $\tilde{\lambda}$ extends the definition of λ to odd links.*

The number $\tilde{\lambda}$ is well-behaved under a change of orientation. Suppose $K_s \in C_r$. Let L_s be the link L with the same orientations on the components except the orientation of K_s reversed. Let $\overline{K_s}$ denote the component K_s with the opposite orientation. Subtracting $\tilde{\lambda}(L) - \tilde{\lambda}(L_s)$, we pick up only the terms where the orientation changes. Thus:

$$\begin{aligned}
\tilde{\lambda}(L) - \tilde{\lambda}(L_s) &= \sum_{1 \le j \le \ell} \left(\widetilde{Lk}(K_s, K_j) - \widetilde{Lk}(\overline{K_s}, K_j) \right) \\
&= \sum_{1 \le j \le \ell} \Big((-1)^{p(K_s,K_j)\cdot\left(Lk(K_s,K_j)+\frac{1}{2}\pi(K_s,K_j)\right)} \\
&\qquad + (-1)^{p(K_s,K_j)\cdot\left(-Lk(K_s,K_j)+\frac{1}{2}\pi(K_s,K_j)\right)} \Big) Lk(K_s, K_j).
\end{aligned}$$

For any j such that $K_j \in C_r$, the term in the sum above becomes $2Lk(K_s, K_j)$. It may be that K_s and K_j interact in an odd number of classical crossings, in which case $2Lk(K_s, K_j)$ may be odd. However, if that happens, it must do so for an even number of such j, because C_r is an even sub-link.

For any j such that $K_j \notin C_r$, the component parity function is given by $p(K_s, K_j) = 1$, and so the exponents come into play. It is still possible that K_s and K_j interact in an even or odd number of classical crossings. If K_s interacts with K_j in an odd number of classical crossings, then $\pi(K_s, K_j) = 1$ and one of the exponents above will be even and the other will be odd. Hence that term will contribute 0. Otherwise, $\pi(K_s, K_j) = 0$ and the exponents will both be even or both be odd. Thus, that term will contribute $\pm 2Lk(K_s, K_j)$, which is an even number, since $Lk(K_s, K_j)$ is an integer in this case.

If $K_r \in M_n$, the argument is similar to the previous case. Hence, these observations, together with Lemma 3.13, prove:

Lemma 3.15. *If L_s is the virtual link obtained from $L = K_1 \cup ... \cup K_\ell$ by reversing the orientation on component K_s then $\tilde{\lambda}(L)$ and $\tilde{\lambda}(L_s)$ differ by an even integer.*

By definition $\tilde{\lambda}$ is possibly a half-integer, and in many cases, an integer. But, in either case the previous lemma guarantees that $(-1)^{\tilde{\lambda}}$ is invariant of the choice of orientation of L, since changing the orientation on a component changes $\tilde{\lambda}$ by an even integer. (Here and throughout the paper, we take $(-1)^{\frac{1}{2}} = \mathrm{i}$.)

Theorem 3.16. *The complex number $(-1)^{\tilde{\lambda}}$ is invariant of the choice of orientation of L.*

We now have all of the ingredients in place to define the *unoriented Jones polynomial* for any virtual link L.

Definition 3.17 (Unoriented Jones Polynomial)**.** *The* unoriented Jones polynomial *for a virtual link L is*

$$\widetilde{J}_L(q) = (-1)^{\left(\tilde{\lambda} - s_- - \frac{1}{2}m\right)} q^{\left(s_+ - 2s_- - \frac{1}{2}m\right)} \langle L \rangle. \tag{8}$$

Note that this definition extends both the definition of the unoriented Jones polynomial for classical links (cf. Equation (4) and Equation (5)) and even links by Remark 3.14. When L is an even virtual link (i.e. when L is its own even core), these two formulas are identical.

As observed in Theorem 3.16, $(-1)^{\tilde{\lambda}}$ need not be a real number, but it turns out that $(-1)^{\tilde{\lambda} - \frac{1}{2}m}$ is. In particular, given a diagram of a virtual link $L = K_1 \cup ... \cup K_\ell$, observe that if $\pi(K_i, K_j) = 1$ then $\widetilde{Lk}(K_i, K_j)$ is a half-integer. If there is an odd number of such pairs, then $\widetilde{\lambda}$ will be a half-integer as well. Otherwise, $\widetilde{\lambda}$ will be an integer. Similarly, in counting the total number of mixed crossings, if there is an odd number of pairs of components such that $\pi(K_i, K_j) = 1$, then

there will be an odd number of mixed crossings in the diagram. Hence, $\frac{1}{2}m$ will be a half-integer in this case, and will be an integer otherwise. In either case, noting that $s_- \in \mathbb{Z}$, we obtain the following lemma.

Lemma 3.18. *For any virtual link L, $\tilde{\lambda} - \frac{1}{2}m \in \mathbb{Z}$, and hence, $(-1)^{\tilde{\lambda}-s_- -\frac{1}{2}m} \in \{-1, 1\}$.*

Theorem 3.19. *The unoriented Jones polynomial, $\widetilde{J}_L$, is an unoriented virtual link invariant. Moreover, $\widetilde{J}_L \in \mathbb{Z}[q^{-\frac{1}{2}}, q^{\frac{1}{2}}]$.*

Proof. The Kauffman bracket clearly does not depend on orientation. The normalization factor $q^{\left(s_+ - 2s_- - \frac{1}{2}m\right)}$ depends only on self-crossings and the total number of mixed-crossings, neither of which change under an orientation switch, and $(s_- + \frac{1}{2}m)$ is orientation invariant for similar reasons. Thus, by Theorem 3.16, the first statement follows.

The second statement follows from Lemma 3.18 and the fact that the polynomial $q^{\left(s_+ - 2s_- - \frac{1}{2}m\right)}\langle L\rangle$ has integer coefficients. □

3.5. Evaluating the unoriented Jones polynomial at 1. In this subsection, we explain why the choices of $(-1)^{-n_-}$ and $(-1)^{\tilde{\lambda}-s_- -\frac{1}{2}m}$ are important normalization factors for the oriented and unoriented Jones polynomials, J_L and $\widetilde{J}_L$. Namely, we will show that evaluating either polynomial at 1 is either 2^ℓ for an ℓ-component even link or 0 if the link is odd. We start with the following definition and lemma.

Definition 3.20. *We define a numerical invariant for virtual links by evaluating the bracket polynomial at 1: $[L] = \langle L\rangle(1)$.*

Observe that $J_L(1) = (-1)^{-n_-}[L]$ and that $\widetilde{J}_L(1) = (-1)^{\tilde{\lambda}-s_- -\frac{1}{2}m}[L]$.

Lemma 3.21. *The usual (oriented) Jones polynomial and unoriented Jones polynomial evaluated at 1 are each invariant under crossing changes. That is, if L_1 and L_2 are oriented virtual links with diagrams that are identical except for a single crossing change, then $J_{L_1}(1) = J_{L_2}(1)$ and $\widetilde{J}_{L_1}(1) = \widetilde{J}_{L_2}(1)$.*

Proof. Consider $\widetilde{J}$ first. The effect of a crossing change on $[L]$ is to multiply by -1. Thus it suffices to show that $\left(\tilde{\lambda} - s_- - \frac{1}{2}m\right)$ changes parity under a crossing change. Suppose c is the crossing to be changed. If c is a self-crossing, then $\tilde{\lambda}$ and m are unaffected (since they only consider mixed crossings), and s_- changes by ± 1.

If c is a mixed crossing then s_- and $\frac{1}{2}m$ remain unchanged. If c involves two components in the same core of L, then the crossing change results in a net change of 1 in the linking number. If the crossing change is between two components that do not belong to the same core, then we consider the effect of the crossing change on $\widetilde{Lk}(K_i, K_j)$ where K_i and K_j are the two components that

cross at c. When the crossing is switched, $Lk(K_i, K_j)$ will change by 1 which is sufficient to change the parity of $\widetilde{Lk}(K_i, K_j)$ as desired.

The proof for J is simpler: changing a positive crossing to a negative (or vice-versa) clearly changes the parity of n_- and hence, compensates for the sign change of $[L]$. □

Remark 3.22. *One possible extension of λ we considered was to use the classical/even λ only on the crossings in the even core(s) and ignore all other crossings. Lemma 3.21 shows why we needed a modified linking number that incorporated every mixed-crossing.*

It is well known that, for a classical link, the usual (oriented) Jones polynomial is, when evaluated at 1, equal to two to the number of components of the link. It was not known how this result extended to virtual links. The following theorem is a new theorem in the (non-classical) virtual link literature.

Theorem 3.23. *If L is an oriented virtual link with ℓ components, then*

$$J_L(1) = \begin{cases} 2^\ell & \text{if } L \text{ is even} \\ 0 & \text{if } L \text{ is odd.} \end{cases}$$

The number, $J_L(1)$, is independent of the choice of orientation.

We first noticed this result in the category of planar trivalent graphs (cf. [1, 3]), and wondered if a similar result held for virtual links. The fact that it does was an important motivation behind this current paper and [2] (See Future Aims, Section 8).

Proof. Enumerate the components of L by $L = K_1 \cup ... \cup K_\ell$. The proof proceeds by induction on the number of classical crossings in the diagram of L. The theorem is clearly true if there are no classical crossings.

Suppose that there exists some crossing for a diagram of L. By repeated applications of Lemma 3.21 we can assume without loss of generality that every crossing of L is positive, i.e., $n_- = 0$. Let c be a (positive) crossing between K_i and some other component K_j of L. If L_A represents the link L with an A-smoothing (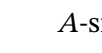) at crossing c, and L_B represents the link L with a B-smoothing (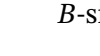) at crossing c, then

$$[L] = [L_A] - [L_B]. \tag{9}$$

Both L_A and L_B have one less component than L since K_i is welded to K_j (see Figure 3).

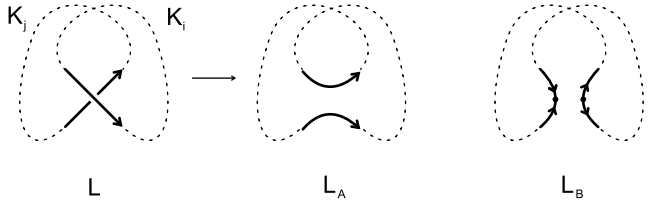

FIGURE 3. Smoothing a crossing.

Observe that if c is oriented as shown on the left side of Figure 3, then the A-smoothing L_A is compatible with this orientation, while the B-smoothing L_B must be reoriented as shown in Figure 4. Let K_{ij} stand for the component in L_B with orientation given by K_j and $\overline{K}_i$, i.e., the part of K_i from L but with the opposite orientation.

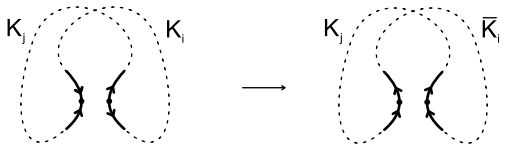

FIGURE 4. Reorienting L_B.

Since $n_- = 0$ for L, $J_L(1) = [L]$. Similarly, $J_{L_A}(1) = [L_A]$. If K_i has $k+1$ classical crossings in L, then after reversing the orientation of K_i in L_B to get an orientation for K_{ij}, the welded K_{ij} component will have k negative crossings in L_B. Thus, $J_{L_B}(1) = (-1)^k[L_B]$. Insert these equations for L, L_A, and L_B into Equation (9) to get

$$J_L(1) = J_A(1) - (-1)^k J_B(1). \tag{10}$$

Note that $(-1)^{k+1} = (-1)^{\pi(K_i)}$. Hence, we can rewrite Equation (10) as

$$J_L(1) = J_A(1) + (-1)^{\pi(K_i)} J_B(1).$$

By induction, $J_A(1)$ must be either $2^{\ell-1}$ or 0 based on the parity of L_A. Similarly, $J_B(1)$ is either $2^{\ell-1}$ or 0 based on the parity of L_B. Moreover, since c is a crossing between two components of L, the parities of L_A and L_B are the same: $\pi(L_A) = \pi(L_B)$. Thus,

$$J_L(1) = \left(1 + (-1)^{\pi(K_i)}\right) 2^{\ell-1} \cdot \pi(L_A).$$

A similar argument applies when the chosen crossing involves only a single component. In that case, L_A and L_B will have an extra component, but the reasoning remains essentially the same. Thus, by induction the theorem follows. □

The proof above is for the usual (oriented) Jones polynomial for virtual links, but the result still holds for the unoriented Jones polynomial. There are two key observations needed to see why this is true. First, by Theorem 3.23, $[L] = 0$

if L is odd. Thus, we need only check $\tilde{J}_L(1)$ for L even. Second, for an even virtual link, $\tilde{\lambda} = \lambda$ (cf. Remark 3.14), and $n_- = -\lambda + s_- + \frac{1}{2}m$. Putting these observations together, we get:

Corollary 3.24. *If L is an unoriented virtual link with ℓ components, then*

$$\widetilde{J}_L(1) = \begin{cases} 2^\ell & \text{if } L \text{ is even} \\ 0 & \text{if } L \text{ is odd.} \end{cases}$$

Therefore, $\tilde{J}_L(1) = J_L(1)$, which means $\tilde{J}_L$ continues to have the same non-negativity propoerty when evaluated at 1 as the (oriented) Jones polynomial J_L.

3.6. Other component parity functions and other polynomials. There are other component parity functions we might have chosen to use in our definition of the modified linking number. Each may be useful in other contexts, though they do not necessarily preserve the properties described in Theorem 3.23 and Corollary 3.24.

The first option is to redefine the parity function so that only components in the even core $C = C_1$ of L evaluate to 0:

$$p_C(K_i, K_j) = \begin{cases} 0 & K_i, K_j \in C \\ 1 & \text{otherwise.} \end{cases}$$

Using this component parity function in the place of p in the definition of the modified linking number leads to a different λ_C and another polynomial J_L^C for which Theorem 3.19 and Corollary 3.24 are both true. While this choice satisfies both of the criteria listed above, the component parity function p is still preferable, as it maximizes the behavior of even links in L.

Another option is to define the parity function to be 1 on every pair of components:

$$p_M(K_i, K_j) = 1 \text{ for all } K_i \text{ and } K_j.$$

Using this parity to define a modified linking number gives rise to a polynomial, J_L^M, for which Theorem 3.19 is still true. However, Corollary 3.24 will fail to be true.

The last option we consider is in some sense the simplest, as it does not use λ, or its variants, at all. The polynomial we obtain from this choice is

$$J_L^0(q) = (-1)^{\left(-s_- - \frac{1}{2}m\right)} q^{\left(s_+ - 2s_- - \frac{1}{2}m\right)} \langle L \rangle. \tag{11}$$

The polynomial is an unoriented virtual link invariant in the sense that it does not require an orientation to define it. It can have complex coefficients, so it does not satisfy the last part of Theorem 3.19, nor does it satisfy Corollary 3.24. Nevertheless, $J_L^0(q)$ has the advantage of being entirely determined by the graded Euler characteristic of the unoriented Khovanov homology described in Section 6.

4. Bracket homology and Khovanov homology

In this section, we briefly describe Khovanov homology along the lines of [4, 22], and we tell the story so that the gradings and the structure of the differential emerge in a natural way. This approach to motivating the Khovanov homology uses elements of Khovanov's original approach, Viro's use of enhanced states for the bracket polynomial [39, 40], and Bar-Natan's emphasis on tangle cobordisms [5].

We begin by working without using virtual crossings, and then introduce extra structure and generalize the Khovanov homology to virtual knots and links in the next section.

A key motivating idea involved in defining the Khovanov invariant is the notion of categorification. One would like to *categorify* the Kauffman bracket $\langle D \rangle$ for a link diagram D of a link L. There are many meanings to the term categorify, but here the quest is to find a way to express the link polynomial as a *graded Euler characteristic* $\langle D \rangle = \chi_q(H(D))$ for some homology theory associated with $\langle D \rangle$. In this section, we define a homology theory with this property. Moreover, the homology theory we define can be used with an orientation on L to get the usual Khovanov homology invariant of L. We call this the *bracket homology of* D and denote it $H(D)$.

The bracket polynomial [16, 17] model for the Jones polynomial [10–12, 41] can be described by the inductive expansion of unoriented crossings  into *A-smoothings*  and *B-smoothings* 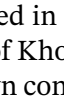 on a link diagram D via Equation 1 and Equation 2: $\langle$ $\rangle = \langle$ $\rangle - q\langle$ $\rangle$ with $\langle \bigcirc \rangle = (q+q^{-1})$. While the bracket polynomial is often described in a variable A, it useful to work with the q-variable version in the context of Khovanov homology.

There is a well-known convention for describing the bracket state expansion by *enhanced states* where an enhanced state has a label of 1 or x on each of its component loops. We then regard the value of the loop $q + q^{-1}$ as the sum of the value of a circle labeled with a 1 (the value is q) added to the value of a circle labeled with an x (the value is q^{-1}).

To see how the Khovanov grading arises, consider the expansion of the bracket polynomial in enhanced states $\mathfrak{s}$:

$$\langle D \rangle = \sum_{\mathfrak{s}} (-1)^{n_B(\mathfrak{s})} q^{j(\mathfrak{s})}$$

where $n_B(\mathfrak{s})$ is the number of B-smoothings in $\mathfrak{s}$, $r(\mathfrak{s})$ is the number of loops in $\mathfrak{s}$ labeled 1 minus the number of loops labeled x, and $j(\mathfrak{s}) = n_B(\mathfrak{s}) + r(\mathfrak{s})$. This can be rewritten in the following form:

$$\langle D \rangle = \sum_{i,j} (-1)^i q^j \dim C^{i,j}(D)$$

where we define $C^{i,j}(D)$ to be the linear span of the set of enhanced states with $n_B(\mathfrak{s}) = i$ and $j(\mathfrak{s}) = j$. Then the number of such states is $\dim C^{i,j}(D)$.

We would like to turn the bigraded vector spaces $C^{i,j}$ into a bigraded complex $(C^{i,j}, \partial)$ with a differential

$$\partial : C^{i,j}(D) \longrightarrow C^{i+1,j}(D).$$

The differential should increase the *homological grading* i by 1 and preserve the *quantum grading* j. Then we could write

$$\langle D \rangle = \sum_j q^j \sum_i (-1)^i \dim C^{i,j}(D) = \sum_j q^j \chi\left(C^{\bullet,j}(D)\right),$$

where $\chi\left(C^{\bullet,j}(D)\right)$ is the Euler characteristic of the subcomplex $C^{\bullet,j}(D)$ for a fixed j. This formula would constitute a type of categorification of the bracket polynomial.

Below, we shall see how *the original Khovanov differential* ∂ *is uniquely determined by the restriction that* $j(\partial \mathcal{s}) = j(\mathcal{s})$ *for each enhanced state* $\mathcal{s}$. Since j is preserved by the differential, these subcomplexes $C^{\bullet,j}$ have their own Euler characteristics and homology. We have $\chi(H^{\bullet,j}(D)) = \chi(C^{\bullet,j}(D))$ where $H^{\bullet,j}(D)$ denotes the bracket homology of the complex $C^{\bullet,j}(D)$. We can write

$$\langle D \rangle = \sum_j q^j \chi(H^{\bullet,j}(D)).$$

The last formula expresses the bracket polynomial as a *graded Euler characteristic*, $\chi_q(H(D))$, of a homology theory associated with the enhanced states of the bracket state summation. This is the desired categorification of the bracket polynomial. Khovanov proved that a gradings-shifted version of this homology theory (using an orientation of the link) is an invariant of oriented knots and links, and that the graded Euler characteristic of the gradings-shifted version is the usual (oriented) Jones polynomial. Thus, he created a new and stronger invariant than the original Jones polynomial.

To define the differential regard two states as *adjacent* if one differs from the other by a single smoothing at some site. Let $(\mathcal{s}, \tau)$ denotes a pair consisting of an enhanced state $\mathcal{s}$ and a site τ of that state with τ of type A. Consider all enhanced states $\mathcal{s}'$ obtained from $\mathcal{s}$ by resmoothing τ from A to B and relabeling (with 1 or x) only those loops that are affected by the resmoothing. Call this set of enhanced states $S'[\mathcal{s}, \tau]$. Define the *partial differential* $\partial_\tau(\mathcal{s})$ as a sum over certain elements in $S'[\mathcal{s}, \tau]$ and the differential for the complex by the formula

$$\partial(\mathcal{s}) = \sum_\tau (-1)^{c(\mathcal{s},\tau)} \partial_\tau(\mathcal{s})$$

with the sum over all type A sites τ in $\mathcal{s}$. Here $c(\mathcal{s}, \tau)$ denotes the number of A-smoothings prior to the A-smoothing in $\mathcal{s}$ that is designated by τ. Priority is defined by an initial choice of order for the crossings in the knot or link diagram.

In Figure 5, we indicate the original forms of the states for the bracket (not yet labeled by 1 or x to specify enhanced states) and their arrangement as a Khovanov category where the generating morphisms are arrows from one state to another where the domain of the arrow has one more A-state than the target of that arrow. In this figure we have assigned an order to the crossings of the

knot, and so the reader can see from it how to define the signs for each partial differential in the complex.

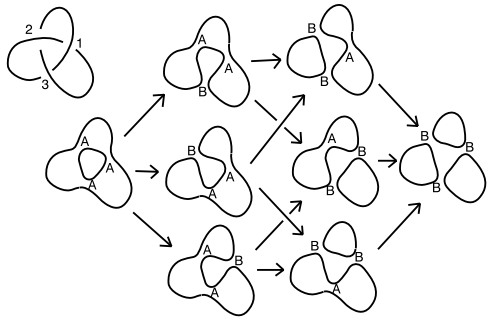

FIGURE 5. Bracket states and Khovanov complex.

We now explain how to define $\partial_\tau(\mathfrak{s})$ so that $j(\mathfrak{s})$ is preserved. The form of the partial differential can be described by the following structure of multiplication and comultiplication on the algebra $V = k[x]/(x^2)$ where $k = \mathbb{Z}$ for integral coefficients:

(1) The element 1 is a multiplicative unit and $x^2 = 0$, and
(2) $\Delta(1) = 1 \otimes x + x \otimes 1$ and $\Delta(x) = x \otimes x$.

These rules describe the local relabeling process for loops in an enhanced state. Multiplication corresponds to the case where two loops merge to a single loop, while comultiplication corresponds to the case where one loop bifurcates into two loops. Thus,

Proposition 4.1. *The partial differentials $\partial_\tau(\mathfrak{s})$ are uniquely determined by the condition that $j(\mathfrak{s}') = j(\mathfrak{s})$ for all $\mathfrak{s}'$ involved in the action of the partial differential on the enhanced state $\mathfrak{s}$.*

We briefly describe how to obtain the usual Khovanov homology from the bracket homology. Let $\{b\}$ denote the degree shift operation that shifts the homogeneous component of a graded vector space in dimension m up to dimension $m + b$. Similarly, let $[a]$ denote the homological shift operation on chain complexes that shifts the rth vector space in a complex to the $(r + a)$th place, with all the differential maps shifted accordingly (cf. [4]). Given an orientation of the link L, the crossings in the diagram D of L can be assigned to be positive or negative in the usual way. If n_+ and n_- are the total number of positive and negative crossings (classical, not virtual), we can shift the gradings of the bracket homology $H(D)$ by $[-n_-]$ and $\{n_+ - 2n_-\}$. Khovanov proved that this shifted bracket homology was an invariant of the oriented link:

Theorem 4.2 (Khovanov, [22])**.** *Let D be a link diagram of an oriented link L. Then*

$$Kh(L) \cong H(D)[-n_-]\{n_+ - 2n_-\}.$$

It is this form of the theory that generalizes nicely to an unoriented version of Khovanov homology (see Section 6).

There is much more that can be said about the nature of the construction of this section with respect to Frobenius algebras and tangle cobordisms. The partial boundaries can be conceptualized in terms of surface cobordisms. The equality of mixed partials corresponds to topological equivalence of the corresponding surface cobordisms, and to the relationships between Frobenius algebras and the surface cobordism category. The proof of invariance of Khovanov homology with respect to the Reidemeister moves (respecting grading changes) will not be given here. See [4, 5, 22]. It is remarkable that this version of Khovanov homology is uniquely specified by natural ideas about adjacency of states in the bracket polynomial.

5. Bracket homology of virtual links

In this section, we describe how to define and calculate Khovanov homology for virtual links for arbitrary coefficients. This section utilizes techniques from [27] and [8], but shows that all of the auxiliary structure (cf. Section 5.1) needed to define the homology emanates from the choice of a single arc-labeled diagram. The arc-labeled diagram turns out to also be perfectly adapted to implementation in a computer algorithm because it encodes the abstract structure of the virtual knot independent of any planar representation (cf. Section 5.3).

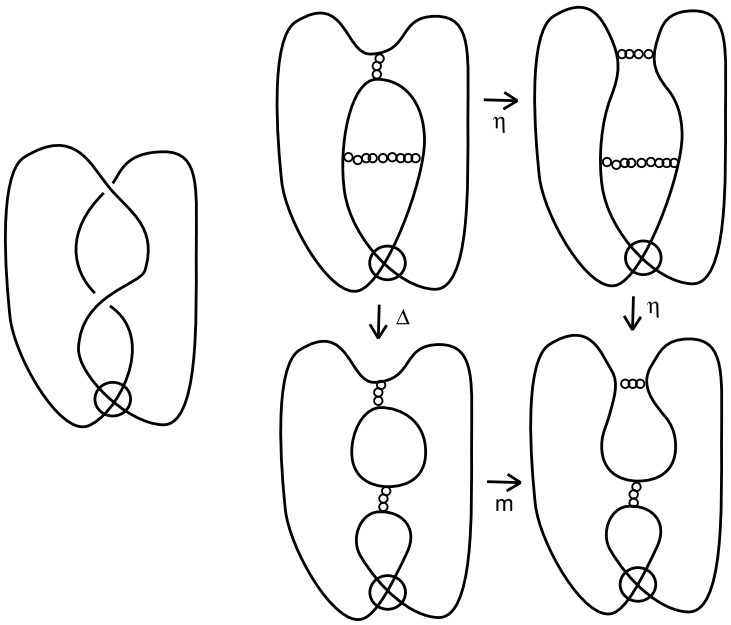

FIGURE 6. Khovanov complex for the two-crossing virtual unknot.

As described in the introduction, extending Khovanov homology to virtual knots for arbitrary coefficients is complicated by the single cycle smoothing as depicted in the first row and second column of Figure 6. We define a map for this smoothing $\eta : V \longrightarrow V$. In order to preserve the quantum grading as in Proposition 4.1, we must have that η is the zero map.

Consider the complex in Figure 6 arising from the 2-crossing virtual unknot. Composing along the top and right we have $\eta \circ \eta = 0$. But composing along the opposite sides we see

$$m \circ \Delta(1) = m(1 \otimes x + x \otimes 1) = x + x = 2x.$$

Hence the complex does not naturally commute or anti-commute.

When the base ring is $\mathbb{Z}/2\mathbb{Z}$ the definition of Khovanov homology given in the previous section goes through unchanged. Manturov [27] (see also [29], [30]) introduced a definition of Khovanov homology for (oriented) virtual knots with arbitrary coefficients. Dye, Kaestner and Kauffman [8] reformulated Manturov's definition and gave applications of this theory. In particular, they found a generalization of the Rasmussen invariant and proved that virtual links with all positive crossings have a generalized four-ball genus equal to the genus of the virtual Seifert spanning surface. The method used in these papers to create an integral version of Khovanov homology involves placing auxiliary structure upon a virtual diagram to make corrections in the local boundary maps so that the individual squares commute. This auxiliary structure includes a base point set, a global order, a local order, and a cut-system.

Our formulation for generating these structures begins by numbering the arcs of a link diagram D, see Figure 7. The arcs of each component are labeled numerically in increasing order. Arc labels change with each pass through a classical crossing. If a component has no classical crossings or only two arcs, stabilize with Reidemeister 1 moves until each component has more than two labeled arcs. This requirement ensures that the increasing order of the arc labels specifies an orientation of the component by traveling along it (see the right hand picture of Figure 7). We summarize these specifications with a definition:

Definition 5.1. *Let L be a virtual link. An* arc-labeled diagram *is an ordered pair (D, A) where D is a link diagram of L and A is a numbering of the arcs of the diagram D such that*

(1) *each arc of each component is labeled numerically in increasing order, changing only when passing through a classical crossing, and*
(2) *the arc labels specify an orientation on each component by following the increasing order of the numbered arcs, i.e., all components have three or more arcs.*

If a link L is oriented and each component of a diagram D of L has three or more arcs, it is possible to choose an arc labeling A for D such that orientation on (D, A) agrees with the orientation of L.

We were motivated to work with arc-labeled diagrams for two reasons. First, and most importantly for this paper, with an arc-labeled diagram one can canonically define a base point set, global order, local order, and cut-system needed to define *integral* Khovanov homology. Second, they are the input needed to define the PD notation of knots used in knot tables (cf. [7,24]), which makes them conducive for encoding knots for computers (see Section 5.3 for a description of PD notation).

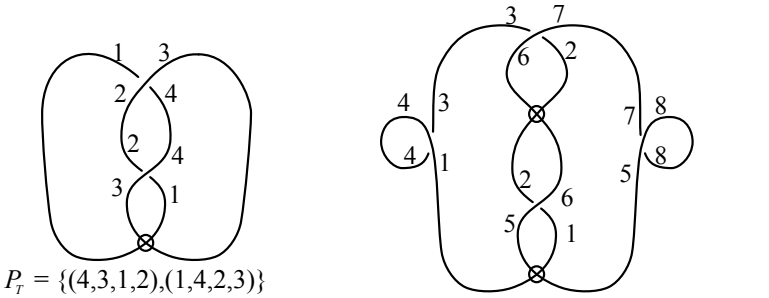

FIGURE 7. A virtual trefoil and a 2-component virtual link with labeled arcs.

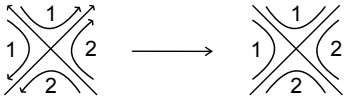

FIGURE 8. The local order determined by the link orientation.

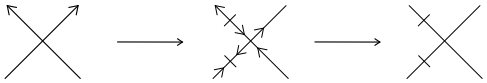

FIGURE 9. Inserting cut-points at the crossings using the canonical source-sink orientation.

5.1. A new auxiliary structure. A diagram with labeled arcs also leads to a natural base point set, global order, local order, and cut-system. Next we show how to build this auxiliary structure from a given arc-labeled diagram, (D, A), of a virtual link L and show that the bracket homology does not depend upon these choices.

Base points: Smoothing each classical crossing results in a merger of two pairs of arcs. With each merger, we label each new arc with the smaller of the two labels. For example, the A-smoothing of the top crossing of the virtual trefoil in

Figure 7 would result in two new arcs now labeled 1 and 3. After smoothing all classical crossings we are left with a collection of immersed circles in the plane, each labeled by the smallest arc in that circle. Since each circle in each state is made up of the labeled arcs from (D, A), including the smallest labeled arc, we can place the base point of [8] on each circle halfway along this smallest labeled arc.

Global order: A global order is a choice of an ordering for each set of circles in a state. By the process described above for base points, each circle in each state has a label given by the smallest arc that forms that circle. An ordering for the set of circles in a state is then given by ordering these labeled circles from least to greatest.

Sign convention for the hypercube: We follow the approach of [27] to put signs on the maps that correspond to edges in the hypercube of states. These signs ensure that each diagram corresponding to a face of the hypercube anti-commutes. First, an exterior algebra-like object (cf. the ordered tensor product in [27]) is created by taking the wedge product of the labeled circles given by the global order. For example, if a state has circles labeled $\{c_1, c_3, c_7, c_9\}$, then form the object $c_1 \wedge c_3 \wedge c_7 \wedge c_9$. The sign of the map corresponding to, say, the merger of circles c_3 and c_9 in this example is determined by an application of the exterior algebra structure with a comparison to the local order of a crossing, as follows: Count the number of transpositions to move each circle to the head of the global order to get $-c_3 \wedge c_9 \wedge c_1 \wedge c_7$. If circle 3 and 9 disagree with the local order (cf. Figure 8) we transpose them; otherwise we do nothing. In this example, suppose c_3 and c_9 disagree with the local order. Thus, we get $c_9 \wedge c_3 \wedge c_1 \wedge c_7$. The circles are then merged to form circle c_3 (since 3 is the smaller label, this will be the corresponding labeled circle in the new state and will locate the base-point on that circle). We then count the number of transpositions required to move c_3 to its position determined by the global order: $-c_1 \wedge c_3 \wedge c_7$. The total number of transpositions used determines the sign to associate to the merger map m. In this example, the number of transpositions is five, so the merger map would be $-m$.

The process for a comultiplication is similar.

Creating a cut-system: As in [8], we place cut points on the diagram to create a source-sink orientation. Unlike [8], we place cut points algorithmically at every classical crossing as shown in Figure 9. They are placed very near the crossing so as not to confuse where the base points are located with respect to the cut points. This is a well-defined cut-system since it is locally well-defined, and away from the classical crossings the source-sink orientation corresponds to that of the orientation of the link given by the arc labels in (D, A).

The source-sink orientation used in Figure 9 is the same as the one used in Figure 11 of [8] at the classical crossings. Whenever our convention places

two cut-points on the same arc, they may be canceled using the first two cut-point moves in Figure 11 of [15]. Thus we obtain a cut-system that is cut-point equivalent to the canonical cut-system of [8].

Remark 5.2. *With the cut-system, base-points and local/global orders so chosen, one may now delete the orientation as in the right hand pictures of Figure 8 and Figure 9. From a diagrammatic perspective, an orientation is no longer required to compute the boundary maps as in Figure 10. However, as described in Question 1.1, it is an open question whether or not this can be accomplished without reference to an orientation.*

Modifying the local boundary maps: Algebra to be processed by the local boundary maps is placed initially at the basepoint of each circle in the state. It is then transferred to the site where the map occurs (e.g. joining two circles at that site or splitting one circle into two at that site). Taking a path along the circle from this basepoint to the site, one will pass either an even number of cut points or an odd number. If the parity is even, then both x and 1 transport to x and 1 respectively. If the parity is odd, then x is transported to $-x$ and 1 is transported to 1. The local boundary map is performed (using the signed map described above) on the algebra, and then in the image state, the resulting algebra is transported back to the base point(s). As above, the path from the site back to the base point will pass through an even or odd number of cut points. The sign of x and 1 at the base point is then determined by this parity according to the same rules above.

Example 5.3. For the arc-labeled diagram of the two-crossing virtual unknot in Figure 10, we show how these choices of global order, local order, base points, and cut point systems work together. In the hypercube of states in Figure 10, we have illustrated the situation where the top left state is labeled with 1 and in the left vertical column we have $-\Delta(1) = -1 \otimes x - x \otimes 1$. We show how the initial element 1 appears at the base point of the upper left state and how it is transported (as a 1) to the site for the co-multiplication. The result of the co-multiplication is $-1 \otimes x - x \otimes 1$ and this is shown at the re-smoothed site. To perform the next local boundary map, we have to transport this algebra to a multiplication site. This result of the co-multiplication is to be transported back to basepoints and then to the new site of multiplication for the next composition of maps. In the figure we illustrate the transport just for $-x \otimes 1$. At the new site this is transformed to $x \otimes 1$. Notice that the $(-x)$ in this transport moves through a single cut-point. We leave it for the reader to see that the transport of $-1 \otimes x$ has even parity for both elements of the tensor product. Thus $-1 \otimes x - x \otimes 1$ is transported to $-1 \otimes x + x \otimes 1$ at the multiplication site. Upon multiplying we have $m(-1 \otimes x + x \otimes 1) = -x + x = 0$. Thus we now have that the composition of the left and bottom sides of the square is equal to the given zero composition of the right and top sides of the square (which is a composition to two zero single cycle maps).

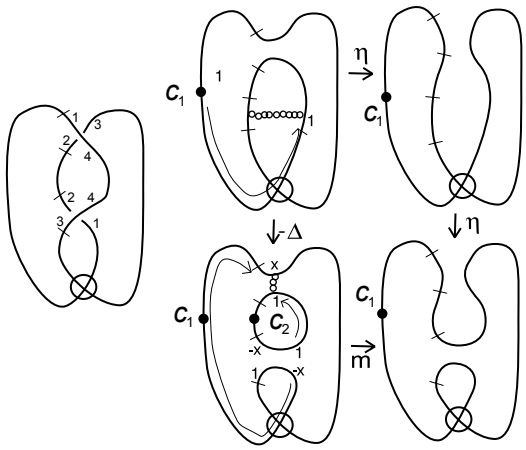

FIGURE 10. Computing the Khovanov complex for the two-crossing virtual unknot.

5.2. Bracket homology. As in Section 4, we can define the chain groups $C^{i,j}(D)$ from the states in the hypercube. The auxiliary structure described above, including the base point set, global order, local order and cut-system allows one to define a differential $\partial^i_A : C^{i,j}(D) \to C^{i+1,j}(D)$. The next theorem shows that $(C^{i,j}(D), \partial_A)$ is a chain complex. We will refer to the homology of this complex as the *bracket homology of* (D, A), and denote it $H(D, A)$.

Theorem 5.4. *Let (D, A) be an arc-labeled diagram for a virtual link L. The arc labels determine a differential*

$$\partial^i_A : C^{i,j}(D) \to C^{i+1,j}(D)$$

and form $(C^{i,j}(D), \partial_A)$ into a chain complex. Furthermore, if A' is another arc labeling for the same diagram D, then $H^{i,j}(D, A) \cong H^{i,j}(D, A')$.

Proof. Given an arc-labeled diagram (D, A), use the numbering on the arcs to define a base point set, global order, local order, and cut-system as described in the paragraphs above. These choices constitute a valid auxiliary structure for computing an integral coefficient homology theory according to [8] (see also [27]). By Theorem 3(2) of [34], any two valid auxiliary structures on the same diagram lead to isomorphic homology theories. □

For a given diagram D of an unoriented virtual link L, the arcs of the diagram can be labeled in different ways. For example, starting with a different arc to label 1 can clearly change the global order. Also, by changing the orientation of the labelings on a component of L, the cut-system and therefore the local order can change. The previous theorem says that the bracket homology does not depend on the choice of arc labeling and therefore it is independent of the choice of the auxiliary structure. It also says that the bracket homology is an invariant of the unoriented link diagram itself (see Remark 5.2). Thus, we may

make the the following definition and work with link diagrams instead of (D, A) from now on.

Definition 5.5. *Given an unoriented link diagram D, label the arcs in order to produce an arc-labeled diagram,* (D, A)*. The chain complex and bracket homology of D is defined to be the chain complex and bracket homology of* (D, A)*, i.e.,*

$$\partial := \partial_A \text{ and } H(D) := H(D, A).$$

While the bracket homology itself is independent of changes in the orientation for a given diagram, calculating it requires the choice of an arc labeling. An arc-labeled diagram automatically comes with an orientation since each component is made up of three or more numerically increasing labeled arcs. The orientation provided allows us to relate the bracket homology to the Khovanov homology by shifting the complex appropriately. Thus we obtain:

Theorem 5.6. *Given two diagrams, D and* D'*, for the same unoriented virtual link L, the bracket homology of each will be isomorphic up to a grading shift. In particular, for some numbers a and b,*

$$H(D) \cong H(D')[a]\{b\}.$$

In particular, if D is a link diagram of an oriented virtual link L, and n_+ *and* n_- *are the number of positive and negative crossings respectively in D, then*

$$H(D)[-n_-]\{n_+ - 2n_-\} \cong Kh(L).$$

Proof. Given two diagrams D and D', choose an arc labeling for each to obtain arc-labeled diagrams (D, A) and (D', A'). The arc labelings give rise to a natural auxiliary structure as outlined in this section, and the arc labelings orient the diagrams. Therefore, by Theorem 3(3) of [34], the bracket homology of each, $H(D)$ and $H(D')$, is isomorphic to the Khovanov homology, with the usual grading shift determined by the orientation. Since the bracket homologies are isomorphic to the Khovanov homology of the link, we obtain that $H(D)$ and $H(D')$ are also isomorphic to each other after an appropriate grading shift (the grading shift accounts for both sequences of Reidemeister moves, as well as a possible change in orientation). □

Note the similarity between Theorem 5.6 and Theorem 4.2. The bracket homology for virtual links defined in this section is a natural extension of the bracket homology for classical links described in Section 4. In the classical case, the two homologies are isomorphic. Other definitions for virtual Khovanov homology have been given by [38] and [36]. Each of these definitions give different solutions to handling the difficult diagram $m \circ \Delta = \eta \circ \eta$ discussed above.

5.3. PD notation and computer programming. The PD notation is a common type of coding of knot diagrams along with Gauss code, Gauss diagrams, and Dowker code (cf. [7, 24]). In this subsection, we show that the PD notation is entirely determined by an arc-labeled diagram (D, A). First, specify a 4-tuple for each classical crossing by recording the arc label of the incoming under-crossing arc and then recording the remaining arc labels in order by going counterclockwise around the crossing (cf. Figure 11). For example, the tuple for the top crossing in the diagram on the left of Figure 7 is $(4, 3, 1, 2)$. The set of all 4-tuples is called the *PD notation* for the link diagram D with labeled arcs and is denoted P. The PD notation of the virtual trefoil diagram with labeled arcs on the left in Figure 7 is $P_T = \{(4, 3, 1, 2), (1, 4, 2, 3)\}$. For comparison, the PD notation for the link diagram with labeled arcs for the link L on the right of Figure 7 is $P_L = \{(3, 4, 4, 1), (1, 6, 2, 5), (2, 7, 3, 6), (7, 5, 8, 8)\}$.

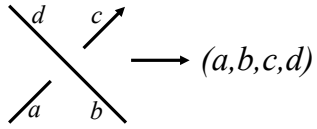

FIGURE 11. Obtaining a 4-tuple for PD notation from a single classical crossing of an arc-labeled diagram.

Since virtual crossings are merely an artifact of the planar representation of a virtual link, it is appropriate that PD notation ignores the virtual crossings, and records only the classical crossings. The set of 4-tuples for the classical crossings determines an arc-labeled diagram up to virtual Reidemeister moves and local isotopy. In this sense, PD notation and arc-labeled diagrams are interchangeable.

Having converted arc-labeled diagrams to a set of 4-tuples, note that the auxiliary structure, and therefore the homology can be derived algorithmically and directly from the PD notation. For example, in any state we know exactly where the base points are and exactly where the cut points are (cf. Figure 9), and therefore one can determine the sign for any path from the basepoint to the smoothing site. The reason why there was no program (since 2007) is that the problem of encoding the needed auxiliary structure seemed insurmountable. Solving the problem of how to produce the auxiliary structure from the arc-labeled diagram (therefore, the PD notation), opened the door to the creation of a new program to compute Khovanov homology. Such a program has been written, and will be described in a subsequent paper.

6. Unoriented Khovanov homology

We are now ready to describe the unoriented Khovanov homology in terms of the bracket homology and a grading shift. Let L be a virtual link and D a diagram of the link. Using Theorem 5.6, the bracket homology $H(D)$ is an invariant of the link up to grading shifts, i.e., given any two diagrams D_1 and D_2

of the same link, there are numbers a and b such that $H(D_1) \cong H(D_2)[a]\{b\}$. While the bracket homology requires the choice of an orientation for computation (though it is independent of that choice), the grading shifts $(-s_- - \frac{1}{2}m)$ and $(s_+ - 2s_- - \frac{1}{2}m)$ needed to define the unoriented Khovanov homology do not require such a choice (see the Introduction and Section 2).

For a diagram D of a link L, shift the bracket chain complex $(C(D), \partial)$ to get the *unoriented Khovanov chain complex*:

$$\tilde{C}(D) = C(D)[-s_- - \frac{1}{2}m]\{s_+ - 2s_- - \frac{1}{2}m\}. \tag{12}$$

We do not include λ, as λ can jump by an even integer by choosing a different orientation. Let $\widetilde{Kh}(D)$ be the homology of this chain complex.

Theorem 6.1. *Let L be an unoriented virtual link, and D_1 and D_2 be two diagrams of L that are equivalent except they differ by one virtual Reidemeister move (virtual or classical). Then $\widetilde{Kh}(D_1) \cong \widetilde{Kh}(D_2)$.*

Proof. For a diagram D of a virtual link L, the homology of the unoriented Khovanov complex $\tilde{C}(D)$ is equal to $H(D)[-s_- - \frac{1}{2}m]\{s_+ - 2s_- - \frac{1}{2}m\}$. By Theorem 5.6, $H(D_1)$ and $H(D_2)$ are isomorphic up to a gradings shift. Therefore, we only need to show that if $\widetilde{Kh}(D_1) \cong \widetilde{Kh}(D_2)[a]\{b\}$, then $a = b = 0$. Since D_1 and D_2 differ by a single Reidemeister move, we check each type of move. Virtual moves V1, V2, V3 and VM (cf. Figure 1) do not effect the enhanced states, s_+, s_-, or m. Hence $\widetilde{Kh}(D_1) = \widetilde{Kh}(D_2)$ in that case. For the first classical Reidemeister move and the second classical Reidemeister move performed on the same component, the terms $-s_-$ and $s_+ - 2s_-$ shift the bracket homology by the same number as in the proof of the oriented Khovanov homology. For the second classical Reidemeister move performed between two different components, $H(D_1) \cong H(D_2)[1]\{1\}$ for the move that removes two mixed-crossings in D_1. In this case, the term $-\frac{1}{2}m$ in both grading shifts compensates for this change in grading. Finally, the third classical Reidemeister move does not change s_+, s_- or m, and it induces an isomorphism $H(D_1) \cong H(D_2)$. In each case, $a = b = 0$, which was to be shown. □

A corollary of this theorem is that $\widetilde{Kh}(D)$ is isomorphic for every diagram D of L. Thus, $\widetilde{Kh}(D)$ is an invariant of L. Therefore, we define:

Definition 6.2. *Let L be an unoriented virtual link and D be a diagram of L. The* unoriented Khovanov homology *of L, denoted $\widetilde{Kh}(L)$, is the homology of the complex $\tilde{C}(D)$.*

Remark 6.3. *The gradings for the chain complex $(C(D), \partial)$ are always integer valued, but the gradings of the shifted unoriented Khovanov chain complex $(\tilde{C}(D), \partial)$ may be half-integer valued.*

For classical links, the gradings of $\tilde{C}(D)$ are always integer valued—there are always an even number of mixed-crossings in a classical link, thus $\frac{1}{2}m$ is always an integer. One might conjecture that the same is true for even links since each component has an even number of mixed-crossings. This is not true, however, as the even virtualized Borromean rings in Figure 12 shows:

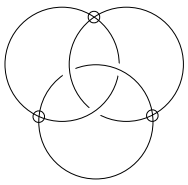

FIGURE 12. An even virtual Borromean Rings with an odd number of mixed-crossings.

Since the homology $\widetilde{Kh}(L)$ can be graded by half-integers, we must extend the usual integral grading to the additive group $\frac{1}{2}\mathbb{Z}$. The graded Euler characteristic for unoriented Khovanov homology is then

$$\chi_q(\widetilde{Kh}(L)) = \sum_{i,j\in\frac{1}{2}\mathbb{Z}} (-1)^i q^j \dim(\widetilde{Kh}^{i,j}(L)).$$

Everything in the formula above continues to make sense if we choose the standard square root of -1, i.e., $(-1)^{\frac{1}{2}} = \mathrm{i}$. The graded Euler characteristic of the unoriented Khovanov homology is a polynomial that may have imaginary valued coefficients. Therefore, evaluating the graded Euler characteristic at 1 is of the form $\mathrm{i}^k \cdot 2^\ell$ for an even virtual link and 0 for an odd link. We could have defined the unoriented Jones polynomial as this graded Euler characteristic, which would yield J^0_L (cf. Equation (11)). For some purposes this could be a reasonable thing to do. However, normalizing the polynomial so that it evaluates to 2^ℓ (even) or 0 (odd) is desirable from the standpoint of matching and generalizing already known theorems in classical link theory. The main motivation behind working with the core and mantle of Section 3.2 was to establish an overall normalization that makes the unoriented Jones polynomial have integer-valued coefficients and evaluates like the oriented Jones polynomial. It is the reason for the extra $(-1)^{\tilde{\lambda}}$ in Equation (8). Thus, up to a well defined "sign," the unoriented Khovanov homology categorifies the unoriented Jones polynomial:

Theorem 6.4. *Let L be a virtual link. Then*

$$\tilde{J}_L(q) = (-1)^{\tilde{\lambda}} \chi_q(\widetilde{Kh}(L)),$$

where $\tilde{\lambda} \in \frac{1}{2}\mathbb{Z}$.

The complex number $(-1)^{\tilde{\lambda}}$, i.e., the "sign," is calculated by choosing an orientation of the virtual link diagram of L, but once computed, the result is independent of the choice of that orientation by Theorem 3.16.

Remark 6.5. *The correction provided by* $(-1)^{\tilde{\lambda}}$ *could be incorporated into the homological grading of* $\tilde{C}(D)$. *Define a function* $\tilde{l}$ *of* $\tilde{\lambda}$ *to the set* $\{0, \frac{1}{2}, 1, \frac{3}{2}\}$ *by*

$$\tilde{l} = \begin{cases} 0 & \text{if } 2\tilde{\lambda} \equiv 0 \pmod 4 \\ \frac{1}{2} & \text{if } 2\tilde{\lambda} \equiv 1 \pmod 4 \\ 1 & \text{if } 2\tilde{\lambda} \equiv 2 \pmod 4 \\ \frac{3}{2} & \text{if } 2\tilde{\lambda} \equiv 3 \pmod 4 \end{cases}$$

The value $\tilde{l}$ *is the same number for any orientation by Theorem 3.16. Replacing* $(-s_- - \frac{1}{2}m)$ *with* $(\tilde{l} - s_- - \frac{1}{2}m)$ *in Equation* (12) *gives an unoriented Khovanov homology whose graded Euler characteristic is* $\tilde{J}_L$.

7. Lee homology of unoriented links

Lee [23] makes another homological invariant of knots and links by using a different Frobenius algebra. She takes the algebra $\mathcal{A} = k[x]/(x^2 - 1)$ with

$$\begin{aligned} x^2 &= 1, \\ \Delta(1) &= 1 \otimes x + x \otimes 1, \\ \Delta(x) &= x \otimes x + 1 \otimes 1, \\ \epsilon(x) &= 1, \\ \epsilon(1) &= 0. \end{aligned}$$

This can be used to define a differential ∂' and a link homology theory that is distinct from Khovanov homology. In this theory, the quantum grading j is not preserved, but *one can use* j *to filter the chain complex for the Lee homology.* The result is a spectral sequence that starts from Khovanov homology and converges to Lee homology.

We can extend Lee's Frobenius algebra to virtual links to get a bracket complex for Lee theory as follows. The involution defined in Section 5 that takes $x \mapsto -x$ as it is transported through a cut point leads to a well-defined, filtered bracket chain complex, $(C'(D), \partial')$, for the algebra $\mathcal{A}$. After shifting overall by the unoriented gradings-shifts presented in this paper, we get a Lee theory for a link that does not require a choice of orientation to define the homology:

Theorem 7.1. *Let* L *be an unoriented virtual link and* D *be any virtual diagram of* L. *The* unoriented Lee Homology $Kh'(L)$, *i.e., the homology of the chain complex*

$$(C'(D)[-s_- - \frac{1}{2}m]\{s_+ - 2s_- - \frac{1}{2}m\}, \partial'),$$

is an invariant of the link L.

The usual (oriented) Lee homology is simple for classical links. One has that the dimension of the Lee homology is equal to 2^ℓ where ℓ is the number of components of the link L (cf. Theorem 3.23). Up to homotopy, Lee's homology has a vanishing differential, and the complex behaves well under link concordance. In his paper [6], Dror BarNatan remarks, "In a beautiful article Eun Soo Lee introduced a second differential on the Khovanov complex of a knot (or link) and showed that the resulting (double) complex has non-interesting homology. This is a very interesting result." Rasmussen [35] uses Lee's result to define invariants of links that give lower bounds for the four-ball genus, and determine it for torus knots. Rasmussen's invariant gives an (elementary) proof of a conjecture of Milnor that had been previously shown using gauge theory by Kronheimer and Mrowka [25, 26].

In [8], Lee homology was generalized to virtual knots and links. Applications of it to unoriented links can be articulated again with the methods of the present paper. We will carry this out in detail in a future paper.

8. Future aims

This paper has been devoted to formulating an unoriented version of the Jones polynomial (via a normalization of the Kauffman bracket polynomial) and a corresponding version of Khovanov homology for virtual knots and links that is an unoriented link invariant. We intend the present paper as a basis for further research and wish to make the following points about future work.

(1) The dependence of the invariant on a choice of orientations is useful in certain contexts. For example, orientations are useful in the context of oriented cobordisms. An invariant of the underlying link is useful as well and may inform on unoriented cobordisms. We will explore the unoriented version of Lee homology for virtual links described above and its applications to cobordisms, genus, and Rasmussen invariants in future research.

(2) This paper grew out of a search for an invariant in a different context: the 2-factor polynomial for ribbon graphs. A ribbon graph G with a perfect matching M can be made to behave like a knot by orienting the cycles in $G \setminus M$ (see for example [1, 3]). However, to define an invariant of a ribbon graph that is independent of the choice of perfect matchings of the graph *and* orientations on the complementary cycles required an "orientation free" invariant. Remarkably, it turns out that the 2-factor polynomial for ribbon graphs corresponds to the unoriented Jones polynomial for virtual links defined in this paper. The integer-valued (not complex-valued) evaluation of the polynomial at 1 turns out to be significant from a graph-theoretic perspective. We explore this idea in [2], and will do more in future papers.

(3) As described in Section 5.3, the authors together with Heather Dye and Aaron Kaestner have constructed a program to calculate the homology theories discussed in this paper using Theorem 5.4. This will appear in a subsequent paper.

At the present time, we know remarkably little about virtual Khovanov homology. It is our intent that this situation will begin to change with the tools developed in this paper.

References

[1] BALDRIDGE, S. A Cohomology Theory for Planar Trivalent Graphs with Perfect Matchings. Preprint, 2018. arXiv:1810.07302. 381, 398

[2] BALDRIDGE, S.; KAUFFMAN, L. H.; RUSHWORTH, W. On ribbon graphs and virtual links. to appear in *European J. Combin.*. arXiv:2010.04238. 381, 398

[3] BALDRIDGE, S.; LOWRANCE, A.; MCCARTY, B. The 2-factor polynomial detects even perfect matchings. *Electron. J. Combin.* **27** (2020), no. 2, P2.27, 16 pp. doi: 10.37236/9214, MR4245082, Zbl 1451.05120, arXiv:1812.10346. 381, 398

[4] BAR-NATAN, D. On Khovanov's categorification of the Jones polynomial. *Algebr. Geom. Topol.* **2** (2002), 337–370. doi: 10.2140/agt.2002.2.337, MR1917056, Zbl 0998.57016, arXiv:math.QA/0201043. 372, 384, 386, 387

[5] BAR-NATAN, D. Khovanov's homology for tangles and cobordisms. *Geom. Topol.* **9** (2005), 1443–1499. doi: 10.2140/gt.2005.9.1443, MR2174270, Zbl 1084.57011, arXiv:math.GT/0410495. 384, 387

[6] BAR-NATAN, D.; MORRISON, S. The Karoubi envelope and Lee's degeneration of Khovanov homology. *Algebr. Geom. Topol.* **6** (2006), 1459–1469. doi: 10.2140/agt.2006.6.1459, MR2253455, Zbl 1130.57012, arXiv:math/0606542. 398

[7] BAR-NATAN, D; MORRISON, S.; ET AL. The Knot Atlas. http://katlas.org. 389, 394

[8] DYE, H. A.; KAESTNER, A.; KAUFFMAN, L. H. Khovanov homology, Lee homology and a Rasmussen invariant for virtual knots. *J. Knot Theory Ramifications* **26** (2017), no. 3, 1741001, 57 pp. doi: 10.1142/S0218216517410012, MR3627701, Zbl 1380.57012, arXiv:arXiv:1409.5088. 367, 369, 387, 388, 390, 391, 392, 398

[9] IM, Y. H.; LEE, K.; LEE, S. Y. Signature, Nullity and Determinant of Checkerboard Colorable Virtual Links. *J. Knot Theory Ramifications* **19** (2010), No. 8, 1093–1114. doi: 10.1142/S0218216510008315, MR2718629, Zbl 1246.57016.

[10] JONES, V. F. R. A polynomial invariant of links via Von Neumann algebras. *Bull. Amer. Math. Soc.* 1985, No. 129, 103–112. doi: 10.1090/S0273-0979-1985-15304-2, MR0766964, Zbl 0564.57006. 384

[11] JONES, V. F. R. Hecke algebra representations of braid groups and link polynomials. *Ann. of Math.* **126** (1987), 335–338. doi: 10.2307/1971403, Zbl 0631.57005, MR0908150. 384

[12] JONES, V. F. R. On knot invariants related to some statistical mechanics models. *Pacific J. Math.* **137** (1989), no. 2, 311–334. Zbl 0695.46029, MR990215. 372, 384

[13] KAMADA, N. Converting virtual link diagrams to normal ones. *Topology Appl.* **230** (2017), 161–171. doi: 10.1016/j.topol.2017.08.032, MR3702763, Zbl 1373.57021. 370

[14] KAMADA, N. Coherent Double Coverings of Virtual Link Diagrams. *J. Knot Theory Ramifications* **27** (2018), No. 11, 1843004. doi: 10.1142/S0218216518430046, MR3868933, Zbl 1401.57018, arXiv:1712.09348. 370, 375, 376

[15] KAMADA, N. Cyclic coverings of virtual link diagrams. *Internat. J. Math.* **30** (2019), No. 14, 1950072. doi: 10.1142/S0129167X19500721, MR4048671, Zbl 1475.57015. 391

[16] KAUFFMAN, L. H. State Models and the Jones Polynomial. *Topology* **26** (1987), 395–407. doi: 10.1016/0040-9383(87)90009-7, MR0899057, Zbl 0622.57004. 372, 384

[17] KAUFFMAN, L. H. "Knots and Physics". World Scientific, Singapore/New Jersey/London/Hong Kong, 1991, 1994, 2001, 2012. MR3013186, Zbl 1266.57001. 384
[18] KAUFFMAN, L. H. Virtual Knot Theory. *European J. Combin.*, **20** (1999), No. 7, 663–691. doi: 10.1006/eujc.1999.0314, MR1721925, Zbl 0938.57006. 373, 374
[19] KAUFFMAN, L. H. A self-linking invariant of virtual knots. *Fund. Math.*, **184** (2004), 135–158. doi: 10.4064/fm184-0-10, MR2128048, Zbl 1064.57004, arXiv:math/0405049. 376
[20] KAUFFMAN, L. H. Virtual Knot Theory–A Concise Summary. To appear in the *Knot Theory Encyclopedia*, CRC/Taylor & Francis. 373
[21] KAUFFMAN, L. H.; TAYLOR, L. R. Signature of Links. *Trans. Amer. Math. Soc.* **216** (1976). doi: 10.1090/S0002-9947-1976-0388373-0, MR0388373, Zbl 0322.55003.
[22] KHOVANOV, M. A categorification of the Jones polynomial. *Duke Math. J.* **101** (2000), no. 3, 359–426. arXiv:math/9908171, doi: 10.1215/S0012-7094-00-10131-7, MR1740682, Zbl 0960.57005. 384, 386, 387
[23] LEE, E. S. An endomorphism of the Khovanov invariant. *Adv. Math.* **197** (2005), No. 2, 554–586. arXiv:math.GT/0210213, doi: 10.1016/j.aim.2004.10.015, MR2173845, Zbl 1080.57015. 397
[24] LIVINGSTON, C.; MOORE, A. H. LinkInfo: Table of Link Invariants, `http://linkinfo.sitehost.iu.edu`, March 4, 2021. 389, 394
[25] KRONHEIMER, P.; MROWKA, T. Gauge Theory for Embedded Surfaces. I. *Topology* **32** (1993), 773–826. doi: 10.1016/0040-9383(93)90051-V, MR1241873, Zbl 0799.57007. 398
[26] KRONHEIMER, P.; MROWKA, T. Gauge Theory for Embedded Surfaces. II. *Topology* **34** (1995), No. 1, 37–97. doi: 10.1016/0040-9383%2894%29E0003-3, MR1308489, Zbl 0832.57011. 398
[27] MANTUROV, V. Khovanov homology for virtual knots with arbitrary coefficients. *J. Knot Theory Ramifications* **16** (2007), No. 3, 345–377. doi: 10.1070/IM2007v071n05ABEH002381, MR2320160, Zbl 1117.57013. 367, 387, 388, 390, 392
[28] MANTUROV, V. Parity and projection from virtual knots to classical knots. *J. Knot Theory Ramifications* **22** (2013), No. 9, 1350044, pp 20. doi: 10.1142/S0218216513500442, MR3105303, Zbl 1280.57007. 376
[29] MANTUROV, V. The Khovanov complex for virtual links. *J. Math. Sci.* **144** (2007), No. 5, 4451–4467. doi: 10.1007/s10958-007-0284-1, Zbl 1165.57012. 388
[30] MANTUROV, V.; ILYUTKO, D. *Virtual Knots: The State of the Art*. Series on Knots and Everything. World Scientific Publishing Co, Hackensack, NJ, 51 edition, 2013. MR2986036, Zbl 1270.57003. 373, 388
[31] MANTUROV, V. Parity in knot theory. *Sb. Math.* **201** (2010), No. 5, 65–110. doi: 10.1070/SM2010v201n05ABEH004089, MR2681114, Zbl 1210.57010. 376
[32] MIYAZAWA, H.; WADA, K.; YASUHARA, A. Linking invariants of even virtual links. *J. Knot Theory Ramifications* **26** (2017), no. 12, 1750072, pp 12. doi: 10.1142/S0218216517500729, MR3718273, Zbl 1404.57016. 370, 375, 376
[33] MORTON, H. The Jones Polynomial for Unoriented Links. *Quart. J. Math. Oxford* **37** (1986), no. 2, 55–60. doi: 10.1093/QMATH/37.1.55, MR0830630, Zbl 0595.57006. 371
[34] NIKONOV, I. Virtual index cocycles and invariants of virtual links. Preprint 2020. arXiv:2011.00248v1. 392, 393
[35] RASMUSSEN, J. Khovanov homology and the slice genus. *Invent. Math.* **182** (2010), No. 2, 419–447. doi: 10.1007/s00222-010-0275-6, MR2729272, Zbl 1211.57009, arXiv:math/0402131. 398
[36] RUSHWORTH, W. Doubled Khovanov homology. *Canad. J. Math.* **70** (2018), no. 5, 1130–1172. doi: 10.4153/CJM-2017-056-6, MR3831917, Zbl 1473.57040. 393
[37] RUSHWORTH, W. A Parity for 2-Colorable Links. Preprint 2020. arXiv:1901.07406. 370, 375, 376, 377

[38] TUBBENHAUER, D. Virtual Khovanov homology using cobordisms. *J. Knot Theory Ramifications*, **9** (2014), No. 23. doi: 10.1142/S0218216514500461, MR3268982, Zbl 1305.57022. 393
[39] VIRO, O. Khovanov homology, its definitions and ramifications. *Fund. Math.* **184** (2004), 317–342. doi: 10.4064/fm184-0-18, MR2128056, Zbl 1078.57013. 384
[40] VIRO, O. Khovanov Homology of Signed Chord Diagrams, unpublished (2006). 384
[41] WITTEN, E. Quantum Field Theory and the Jones Polynomial. *Comm. Math. Phys.* **121** (1989), 351–399. doi: 10.1007/BF01217730, MR0990772, Zbl 0667.57005. 384

(Scott Baldridge) DEPARTMENT OF MATHEMATICS, 303 LOCKETT HALL, LOUISIANA STATE UNIVERSITY, BATON ROUGE, LA 70803, USA
baldridge@math.lsu.edu

(Louis H. Kauffman) DEPARTMENT OF MATHEMATICS, STATISTICS AND COMPUTER SCIENCE, 851 SOUTH MORGAN STREET, UNIVERSITY OF ILLINOIS AT CHICAGO, CHICAGO, ILLINOIS 60607-7045, USA, AND DEPARTMENT OF MECHANICS AND MATHEMATICS, NOVOSIBIRSK STATE UNIVERSITY, NOVOSIBIRSK, RUSSIA
kauffman@uic.edu

(Ben McCarty) DEPARTMENT OF MATHEMATICAL SCIENCES, 373 DUNN HALL, UNIVERSITY OF MEMPHIS, MEMPHIS, TN 38152, USA
ben.mccarty@memphis.edu

This paper is available via http://nyjm.albany.edu/j/2022/28-14.html.